

## Article

# Hemp FRRP Confined Lightweight Aggregate Concrete (LWAC) Circular Columns: Experimental and Analytical Study

Suniti Suparp<sup>1</sup>, Krisada Chaiyasarn<sup>2</sup>, Nazam Ali<sup>3</sup>, Chaitanya Krishna Gadamma<sup>4</sup>,  
Ahmed W. Al Zand<sup>5</sup>, Ekkachai Yooprasertchai<sup>6</sup>, Qudeer Hussain<sup>7</sup>, Panuwat Joyklad<sup>1,\*</sup>  
and Muhammad Ashraf Javid<sup>8</sup>

<sup>1</sup> Department of Civil and Environmental Engineering, Faculty of Engineering, Srinakharinwirot University, Nakhonnayok 26120, Thailand

<sup>2</sup> Thammasat Research Unit in Infrastructure Inspection and Monitoring, Repair and Strengthening (IIMRS), Faculty of Engineering, Thammasat School of Engineering, Thammasat University Rangsit, Klong Luang, Pathumthani 12000, Thailand

<sup>3</sup> Department of Civil Engineering, University of Management and Technology, Lahore 54770, Pakistan

<sup>4</sup> Structural Engineering, Asian Institute of Technology (AIT), School of Engineering and Technology (SET), Pathumthani 12120, Thailand

<sup>5</sup> Department of Civil Engineering, Universiti Kebangsaan Malaysia (UKM), Bangi 43600, Malaysia

<sup>6</sup> Construction Innovations and Future Infrastructure Research Center (CIFIR), Department of Civil Engineering, Faculty of Engineering, King Mongkut's University of Technology Thonburi, Bangkok 10140, Thailand

<sup>7</sup> Center of Excellence in Earthquake Engineering and Vibration, Department of Civil Engineering, Chulalongkorn University, Bangkok 10330, Thailand

<sup>8</sup> Department of Civil Engineering, NFC Institute of Engineering and Fertiliser Research, Faisalabad 38090, Pakistan

\* Correspondence: panuwatj@g.swu.ac.th



**Citation:** Suparp, S.; Chaiyasarn, K.; Ali, N.; Gadamma, C.K.; Al Zand, A.W.; Yooprasertchai, E.; Hussain, Q.; Joyklad, P.; Javid, M.A. Hemp FRRP Confined Lightweight Aggregate Concrete (LWAC) Circular Columns: Experimental and Analytical Study. *Buildings* **2022**, *12*, 1357. <https://doi.org/10.3390/buildings12091357>

Academic Editors: Gaochuang Cai, Amir Si Larbi, Konstantinos Daniel Tsavdaridis and Nerio Tullini

Received: 5 July 2022

Accepted: 29 August 2022

Published: 1 September 2022

**Publisher's Note:** MDPI stays neutral with regard to jurisdictional claims in published maps and institutional affiliations.



**Copyright:** © 2022 by the authors. Licensee MDPI, Basel, Switzerland. This article is an open access article distributed under the terms and conditions of the Creative Commons Attribution (CC BY) license (<https://creativecommons.org/licenses/by/4.0/>).

**Abstract:** Intrinsically, lightweight aggregate concrete (LWAC) suffers from the low compressive strength and deformation capacity. This restricts the use of LWAC mainly to non-structural applications. Several studies have highlighted the potential of synthetic fiber-reinforced polymer (FRP) jackets for improving the substandard properties of the LWAC. However, the high costs associated with FRP jackets are generally a concern. This study identifies hemp fiber-reinforced rope polymer (FRRP) wraps as a potential alternative to the synthetic FRP jackets. The salient features of hemp FRRP include its low cost and easy availability. Therefore, the main question that needs to be answered is: can hemp FRRP strengthen LWAC as a low-cost alternative to synthetic FRP jackets? To quantitatively explain the effects of lightweight aggregates on concrete compressive strength, 24 concrete cylinders were tested in three groups. Group 1, 2, and 3 cylinders comprised 0, 50, and 100% of lightweight aggregates as natural aggregate replacements. The peak stress of the concrete was reduced by 34% and 49% in the presence of 50% and 100% lightweight aggregates, respectively. It was concluded that a single layer of hemp FRRP on Group 2 cylinders (i.e., 50% aggregate replacement) was sufficient to enhance the peak stress to the same level as that of the control cylinder in Group 1 (i.e., fabricated using natural aggregates only). At the same time, it took two layers of external FRRP on Group 3 cylinders to achieve the same strength. A positive correlation between the peak stress of the LWAC and the number of hemp FRRP layers was observed. Nonetheless, Group 1 and 3 cylinders formed the upper and lower bounds in terms of peak stress for the same level of confinement. Further to the interest, three layers of hemp FRRP shifted brittle compressive stress–strain response to a bi-linear response for all amounts of lightweight aggregates. Several existing analytical peak stress models were assessed in predicting the experimental results. From the results, it was inferred that none of these models predicted the compressive strength of all three groups of cylinders consistently.

**Keywords:** hemp fiber rope; fiber-reinforced polymer composites; lightweight aggregate concrete; axial compression; strength models

## 1. Introduction

Lightweight aggregate concrete (LWAC) can be characterized as high-performance concrete comprising aggregates with high porosity and low bulk density. It furnishes a unique distribution of the content of air voids both within the aggregates and inside the concrete matrix. Moreover, the interfacial bond between aggregates and the matrix is governed by the amount of aggregate particle saturation [1]. Among its various advantages, it includes a high strength-to-weight ratio, enhanced fire resistance, and reduced magnitudes of dead loads [2]. A significant concern regarding LWAC arises from their low-grade deformation capacity and brittle behavior [3].

Over the years, applications of the LWAC for structural purposes can be found which can be attributed to its excellent properties [4–7]. However, with 30–35% lower weight, the strength properties of LWAC are relatively low compared to natural aggregate concrete (NAC) [8]. Moreover, issues related to its high creep and shrinkage, brittleness, and low elastic modulus properties have restricted its applications to well below its potential [9]. There is no question that the lightweight nature of the comprising aggregates reduces LWAC's density. However, this is often accomplished at the expense of reduced ductility and compressive strength [10]. Therefore, LWAC often finds its use in non-structural components, and its potential in the fabrication of columns, beams, and other load-bearing elements limited.

Coarse aggregates comprising LWAC are susceptible to fracture, thus causing different and earlier failure than those found in NAC. This can be reverted if sufficient lateral confinement pressure is applied to improve the synergistic influence between lightweight aggregates and cement matrix [11]. Khaloo et al. [12] investigated the effect of external confinement in the form of single hoops or interlocking double spiral hoops on the axial performance of lightweight concrete columns. It was demonstrated that the steepness of the post-peak axial stress vs. strain response became mild, thus exhibiting higher ductility than that of the control column. Recently, fiber-reinforced polymers (FRPs) have been utilized in structural strengthening works for numerous benefits, including their noticeable strength-to-weight ratio, corrosion endurance, low self-weight, durability, and good design ability [13]. Recognizing these benefits, a host of research has been conducted to explore the axial compressive behavior of FRP-confined concrete from monotonic stress–stress behavior [3,14–16] to cyclic behavior [17–19]. Despite possessing many brilliant features, the high costs of synthetic FRPs and resins are an evident and inevitable concern [20]. Moreover, synthetic chemicals are employed in the fabrication of the conventional FRPs. Direct exposure to uncured resins, hardeners, or FRP dust may cause skin problems including irritation and allergic contact dermatitis to the users [21–24].

The remedy lies in the replacement of these synthetic fibers with the natural fibers [25]. Recently, Hussain et al. [26] introduced a novel technique using inexpensive and sustainable fiber rope-reinforced polymer (FRRP) composites for enhancing the peak compressive strength, the ultimate strain, and compressive ductility of the plain concrete. Hemp, cotton, and polyester ropes were used to wrap cylindrical concrete specimens in different layers to assess the FRRP confinement magnitude. Among the considered FRRP composites, it was inferred that hemp FRRP imparted maximum peak compressive strength gain to the plain concrete specimens. From these results, it may be expected that the confinement mechanism of hemp FRRP will impart similar improvements in the case of LWAC. Recently, Suparp et al. [27] improved the peak compressive stress and the ductility of the lightweight aggregate concrete with square sections using hemp fiber rope confinement. A significant improvement in both the peak compressive stress and the ultimate strain was observed, indicating the efficacy of the hemp fiber rope in mitigating substandard compressive characteristics of the lightweight aggregate concrete. Hussain et al. [28] strengthened shear critical RC beams using hemp FRRP wraps. The strengthening of shear critical beams using hemp FRRP wraps was found to be an effective solution to mitigate the shear failures. Beams strengthened with hemp FRRP demonstrated up to 63% higher load carrying capacity as compared to the reference beam. Joyklad et al. [29] strengthened axial

compression deficient recycled aggregate concrete (RAC) cylinders using one, two, and three wraps of hemp FRRP. A significant improvement in the peak compressive strength and axial ductility of hemp FRRP-strengthened LWAC cylinders was observed, where a bi-linear axial stress–strain response was observed for three-layer strengthened LWAC cylinders. Hussain et al. [30] examined the effectiveness of hemp rope confinement on square plain concrete specimens with corner radius as a major parameter. The gain in compressive strength was found to be proportional to the size of the corner radius.

To date, no study has been conducted on the strengthening of circular LWAC sections using hemp FRRP wraps. Based on the performance of hemp FRRP in strengthening applications, its use in strengthening LWAC with circular sections would be an effective solution. Further, hemp fibers have a massive market worldwide and its easy availability around the globe makes it a suitable alternative to the synthetic FRP jackets. It was reported that the gross area of hemp cultivation in Europe was increased by 70% from 2013–2018 and the number of its hectares jumped by 614% in the year 2018 as compared to the year 1998 [31]. Therefore, this study intends to find the potential benefits of hemp FRRP in improving the axial stress–strain constitutive parameters of LWAC circular columns, such as peak compressive strength, its corresponding strain, elastic modulus, and post-peak degradation response. Further, the number of external hemp FRRP wraps is identified as a potential factor in addressing the compressive stress vs. strain behavior of the hemp FRRP confined concrete. This study will be helpful to enrich the database of hemp FRRP confined LWAC circular columns and adds to the possible use of LWAC as commercial concrete.

## 2. Experimental Program

### 2.1. Test Matrix

Experiments were performed on 24 cylinders, each measuring 150 mm × 300 mm (diameter to height). The size effect is an important factor affecting the confinement effectiveness of the concrete columns. In the previous studies, the effectiveness of FRP wraps to enhance ultimate strength was found to be higher for short columns than slender columns [26,27]. However, the size effect was not considered in this study and a constant height was considered for all specimens. There were two main parameters of interest in this study, i.e., the quantity of lightweight aggregates and the amount of external confinement in the form of hemp FRRP layers. Their interaction was considered in this study by systematically arranging them into three groups, as shown in Table 1. Specimens in Group 1 were constructed using NAC only, comprising one control specimen and three specimens strengthened using different hemp layers. For instance, specimens 2, 3, and 4 were strengthened using one, two and three layers of hemp FRRP, respectively. Further, two specimens were constructed corresponding to each specimen type. Thus, eight specimens were experimented on in the first group. Groups 2 and 3 comprised a similar test matrix to that of Group 1 with the only difference being the presence of the LWAC. Specimens in Groups 2 and 3 were constructed by substituting 50% and 100% of natural aggregates for lightweight aggregates, respectively. A three-part nomenclature was adopted to represent specimens identifying their group and sub-group. The first letter “C” was common for all specimens representing “cylinder” followed by a number, i.e., 0, 50, or 100. This number represented the percentage (%) quantity of lightweight aggregates that were used in the construction of that specimen. Finally, the third letter, i.e., 1H, 2H, or 3H, represented the number of external hemp FRRP layers. For instance, the name C-50-2H corresponds to the cylinder that contained 50% natural and 50% of lightweight aggregates in its concrete mix and was strengthened using two layers of hemp FRRP.

**Table 1.** Test matrix.

| Group | Specimen  | Quantity of Lightweight Aggregates (%) | Number of Layers of Hemp FRP | Number of Specimens |
|-------|-----------|--|------------------------------|---------------------|
| 1     | C-0-CON   | 0                                      | 0                            | 2                   |
|       | C-0-1H    | 0                                      | 1                            | 2                   |
|       | C-0-2H    | 0                                      | 2                            | 2                   |
|       | C-0-3H    | 0                                      | 3                            | 2                   |
| 2     | C-50-CON  | 50                                     | 0                            | 2                   |
|       | C-50-1H   | 50                                     | 1                            | 2                   |
|       | C-50-2H   | 50                                     | 2                            | 2                   |
|       | C-50-3H   | 50                                     | 3                            | 2                   |
| 3     | C-100-CON | 100                                    | 0                            | 2                   |
|       | C-100-1H  | 100                                    | 1                            | 2                   |
|       | C-100-2H  | 100                                    | 2                            | 2                   |
|       | C-100-3H  | 100                                    | 3                            | 2                   |

## 2.2. Material Properties

Portland cement of Type-I was used in the concrete mix of all specimens. Locally available fine aggregates from river sand were used. The maximum size of coarse aggregates was limited to 25 mm. Lightweight aggregates were provided by INSEE Thailand, and their nominal size ranged from 12–18 mm. Table 2 provides the quantity of each material for the concrete mix of each group. Figure 1 presents lightweight aggregates used in this study.

**Table 2.** Concrete mix proportions.

| Quantity (kg/m <sup>3</sup> ) | Group-1 | Group-2 | Group-3 |
|-------------------------------|---------|---------|---------|
| Cement                        | 600     | 600     | 600     |
| Fine aggregates               | 600     | 600     | 600     |
| Natural coarse aggregates     | 900     | 450     | 0.0     |
| Lightweight aggregates        | 0.0     | 450     | 900     |
| Water                         | 300     | 300     | 300     |
| Slump (cm)                    | 8       | 8       | 8       |

**Figure 1.** Lightweight aggregates.

### 2.3. Construction of Test Specimens

Cylinders were constructed in the laboratory conditions. Steel molds were used to cast cylinders. Each mold was filled in three equal layers. Molds were placed on a vibration table during concrete pouring. The vibration was imparted to molds after each concrete layer pouring. Molds were removed after one day of casting, whereas curing was continued for 28 days in the laboratory environment. Wrapping of cylinders using hemp ropes was initiated at one end. The last part of the hemp rope was attached to the concrete to avoid unnecessary movement. After that, the polyester resin was employed to the surface using a hand brush. Hemp ropes (Figure 2) were subsequently bonded to the concrete surface. The polyester resin was again brushed onto the wrapped hemp ropes to form a composite. For specimens strengthened with more than one hemp FRRP layer, a similar procedure was implemented to bond additional layers to the underlying layers. Special care was practiced to avoid any gap between adjacent hemp ropes within a single wrap.



**Figure 2.** Hemp fiber rope.

### 2.4. Load Setup and Instrumentation

Each cylinder was exposed to monotonic compressive load using a universal testing machine (UTM). Before placing cylinders in the UTM, their top and bottom surfaces were cleaned, and rough patches were smoothed, ensuring the uniform application of the compressive loads. Then, a circular steel plate was fixed to the top surface, which improved the concentration of the load. Linear variable differential transducers (LVDTs) were used for the continuous monitoring of axial displacements. LVDTs were pre-calibrated before the test. LVDTs were mounted on the bottom steel plate, whereas the tip was attached to the loading plate of UTM, as indicated in Figure 3.

Figure 4 presents the typical test configuration implemented to measure the tensile stress vs. strain characteristics of the hemp fiber ropes. A monotonic tensile load was applied to hemp FRRP by a universal testing machine (UTM) with a 200 Ton capacity. Load was applied through a controlled loading setup at a speed of 4 kN/s. Two steel plates were attached to the top and bottom surface of each specimen before the test was started to ensure and guarantee the uniform application of the load. The magnitude of the load was measured using a load cell, as illustrated in Figure 3. The fracture tensile capacity of the hemp FRRP was approximated at 750 N at an average extension of 2.21 mm.

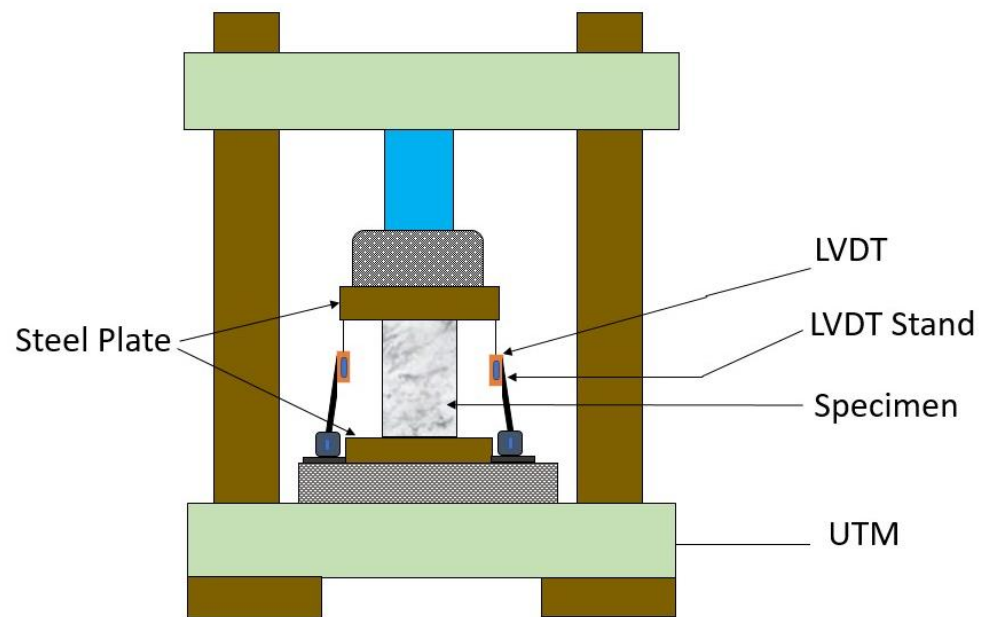


Figure 3. Test setup and instrumentation.

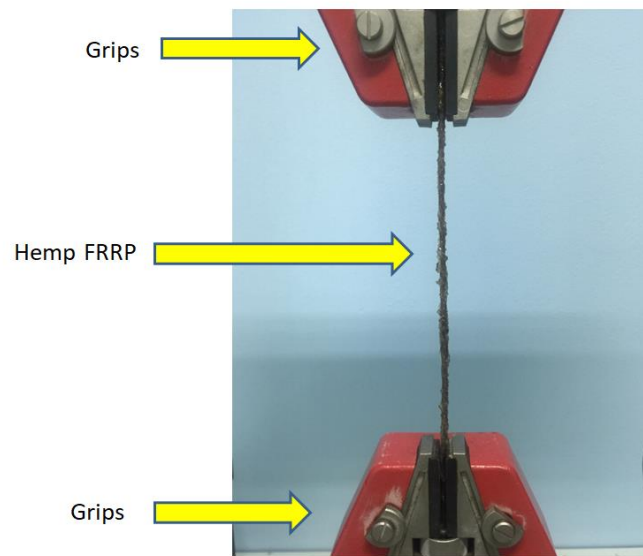
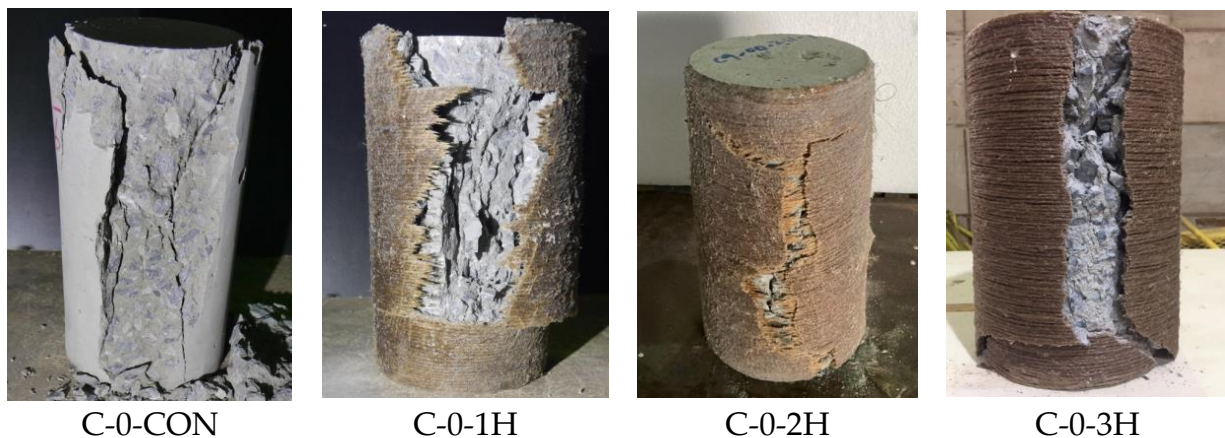


Figure 4. Test setup of hemp FRRP.

### 3. Experimental Results

#### 3.1. Ultimate Failure Modes

Group 1: Figure 5 shows the ultimate failure modes observed for concrete cylinders of Group 1. Group 1 cylinders did not incorporate lightweight aggregates. Control cylinder C-0-CON failed in a typical manner, suddenly forming cones and exhibiting splitting along its height. Splitting alongside failure cones indicated that the plates of the test apparatus did not provide friction to restrict the lateral expansion near cylinder ends. Cylinder C-0-1H was confined with a single layer of hemp FRRP. Under the large circumferential expansion of the cylinder, hoop stresses of high magnitudes were generated in hemp FRRP. Ultimately, hemp FRRP failed under these hoop stresses when their magnitudes surpassed the inherited tensile capacity of hemp FRRP. The resulting failure was brittle and explosive that propagated almost along the full height of the cylinder. Cylinders confined with two and three layers of hemp FRRP also demonstrated splitting of the hemp FRRP along their heights.



**Figure 5.** Failure modes of concrete prisms (Group 1).

Group 2: Typical failures of Group 2 cylinders are presented in Figure 6. Unlike Group 1 cylinders, Group 2 specimens were constructed by substituting 50% of the natural aggregates with lightweight aggregates. The consequences are reflected in their failure mechanisms, as shown in Figure 6. Foremost, control cylinder C-50-CON failed by crushing and splitting like its counterpart cylinder in Group 1. However, its failure cone was significantly shifted towards its top end, as highlighted in Figure 6. This may be ascribed to the modest density of lightweight aggregates as compared to that of natural aggregates. It was expected that during the vibration of wet concrete after its placement in molds, lightweight aggregates were separated from natural aggregates and floated above them. This resulted in a failure cone with the apex shifted towards the top surface. For the cylinder strengthened with a single hemp FRRP layer, i.e., C-50-1H, failure accompanied the tensile rupture of hemp FRRP within the top half. For cylinders strengthened with two and three layers, tensile fracture of hemp FRRP spread vertically, as shown in Figure 6.

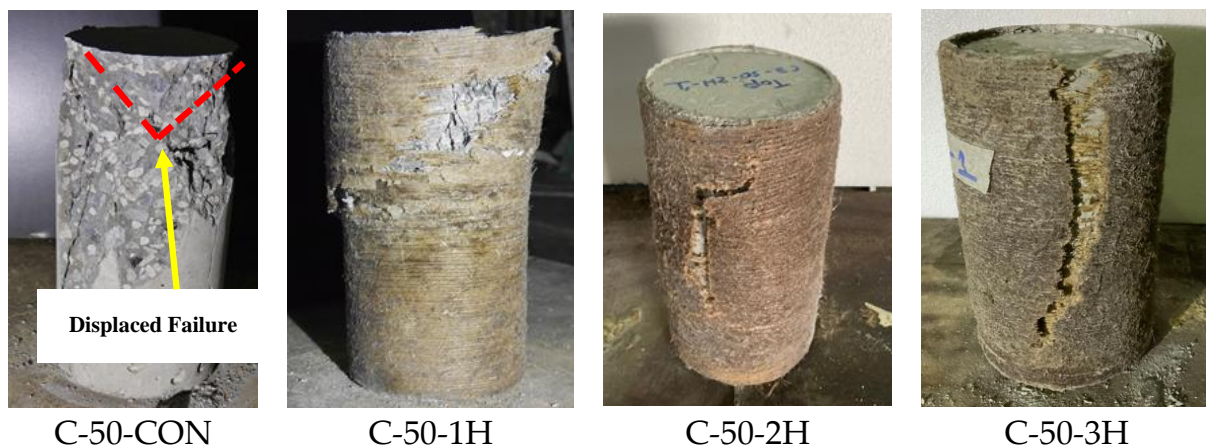


**Figure 6.** Failure modes of concrete prisms (Group 2).

Group 3: Group 3 cylinders were constructed with lightweight aggregates (i.e., 100% replacement of the natural aggregates). Crushing of concrete was detected in the vertical direction of the control cylinder C-100-CON. The cylinder confined with a single hemp FRRP layer demonstrated tensile rupture of the external confinement near the loading surface. It is to be mentioned that no additional measure was taken to constrain hemp FRRP at both ends of the cylinders. For heavier confinements, i.e., two and three hemp FRRP layers, tensile rupture of hemp FRRP at large lateral deformations determined the ultimate failure. Failure types of Group 3 cylinders are displayed in Figure 7.



**Figure 7.** Failure modes of concrete prisms (Group 3).

### 3.2. Ultimate Load and Strain

One of the key features of external wraps is to enhance concrete inherited compressive strength and the corresponding strain. Cylinders strengthened with hemp FRRP exhibited both these enhancements. Table 3 summarizes the peak stress and the ultimate strain of the cylinders. As stated in earlier sections, two cylinders were cast for each cylinder type. Hence, the results reported in this section are averages of the two representative cylinders for each category.

**Table 3.** Summary of peak compressive stress and corresponding strain.

| Group | Specimen  | Peak Stress (MPa) | Increase in Peak Stress (%) | Ultimate Strain | Ultimate Strain (%) |
|-------|-----------|-------------------|-----------------------------|-----------------|---------------------|
| 1     | C-0-CON   | 24.90             | -                           | 0.0045          | -                   |
|       | C-0-1H    | 38.48             | 55                          | 0.0056          | 24                  |
|       | C-0-2H    | 49.24             | 98                          | 0.0067          | 49                  |
|       | C-0-3H    | 65.34             | 162                         | 0.0251          | 458                 |
| 2     | C-50-CON  | 16.41             | -                           | 0.0051          | -                   |
|       | C-50-1H   | 25.18             | 53                          | 0.0059          | 16                  |
|       | C-50-2H   | 26.83             | 63                          | 0.0066          | 29                  |
|       | C-50-3H   | 39.33             | 140                         | 0.0288          | 465                 |
| 3     | C-100-CON | 12.73             | -                           | 0.0042          | -                   |
|       | C-100-1H  | 19.24             | 51                          | 0.0046          | 10                  |
|       | C-100-2H  | 23.20             | 82                          | 0.0050          | 19                  |
|       | C-100-3H  | 29.58             | 131                         | 0.0236          | 463                 |

As presented in Table 3, the effect of lightweight aggregates on concrete compressive strength cannot be neglected. The presence of lightweight aggregates by replacing 50% and 100% of natural aggregates reduced the compressive strengths by 34% and 49%, respectively (corresponding to the compressive strengths of 16.41 and 12.73 Mpa for C-50-CON and C-100-CON, respectively, as opposed to the compressive strength of 24.90 Mpa for C-0-CON).

For cylinders in Group 1, the compressive strength increased by 55%, 98%, and 162% for one, two, and three wraps of hemp FRRP, respectively. Although a substantial rise in the peak stress was noted for single and double layers of the hemp FRRP, results suggested that an increase in equivalent magnitude was not detected for the corresponding strain values. This is reflected by a mere increase of 24% and 49% enhancement in the ultimate strain corresponding to single and double hemp FRRP layers. Nonetheless, a substantial enhancement in the ultimate strain was noted for the three-layer wrap, i.e., a 458% increase in the ultimate strain of cylinder C-0-3H over that of cylinder C-0-CON.

For cylinders in Group 2, peak stress for one, two, and three hemp FRRP layers increased by 53%, 63%, and 140%, respectively, over that of their corresponding control cylinder, i.e., C-50-CON. At the same time, corresponding strain values increased by 16%,

29%, and 465%, respectively. This improvement in the peak stress and the ultimate strain as a result of hemp confinement was found to be consistent with their counterpart values of Group 1 cylinders. Cylinders of Group 3 also exhibited a similar trend in their improvements of the compressive strength and ultimate strains as a result of hemp confinement.

An interesting observation is plotted in Figure 8. Cylinders of Group 1 (i.e., consisting only of natural aggregates) created the upper bound in terms of compressive strength for all confinement configurations. On the contrary, cylinders of Group 3 formed the lowest bound. It is interesting to observe that lightweight aggregates deduced a sufficient amount of compressive strength, and this deduction increased as the amount of lightweight aggregates is increased. Though a considerable enhancement in the peak stress was accomplished for Group 2 and 3 cylinders, this increase could never fill the gap that was created by the presence of lightweight aggregates, even in the case of three-layer hemp FRRP wrap. It is mentioned that a similar amount of improvement in peak stress to those in Groups 1 and 3 was not observed when specimens in Group 2 were confined by two layers of hemp FRRP. This is ascribed to the personal error caused during the wrapping and impregnation of hemp FRRP layers.

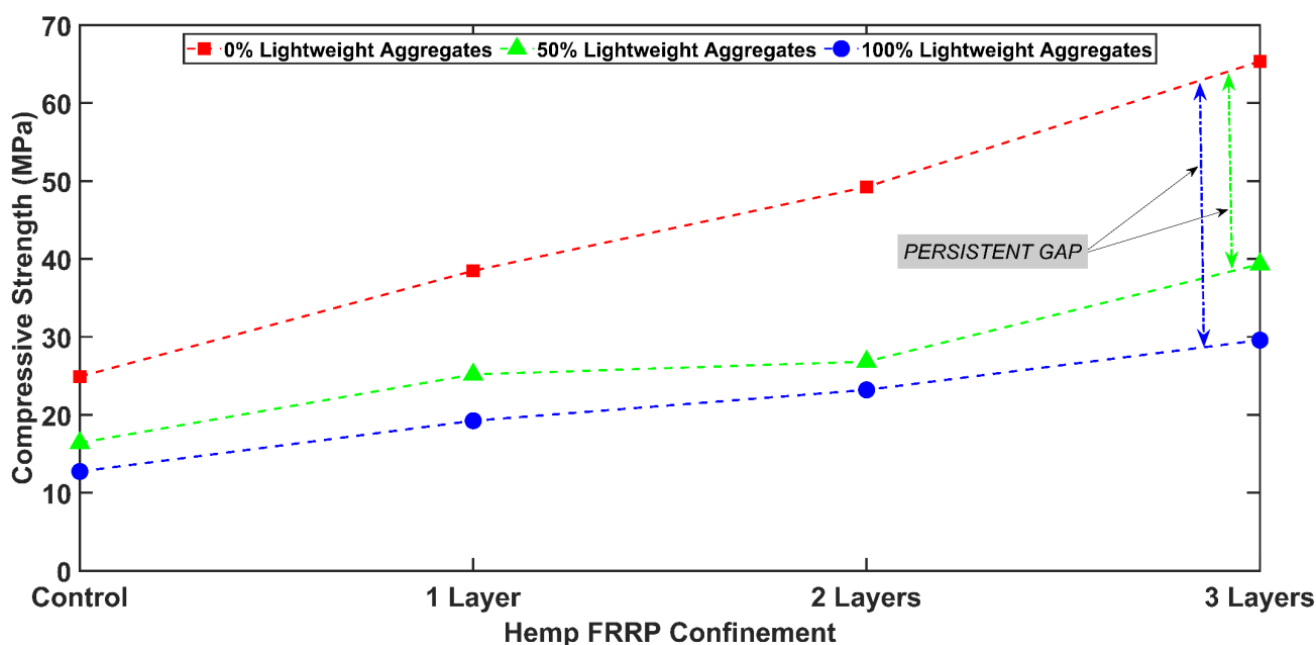


**Figure 8.** Comparison of the compressive strengths between different groups (function of the amount of hemp FRRP).

### 3.3. Stress–Strain Curves

Figure 9 contains the compressive stress versus the corresponding strain response of Group 1 cylinders. The control cylinder formed the lowest bound in terms of the peak strength. Its characteristic stress vs. strain response included a linear increasing branch succeeded by a sudden fall. The brittle behavior was associated with the control cylinder. Confining cylinders with hemp fibers increased the peak stress and strain and improved the post-peak response. A gradual transition from brittle in the control cylinder to a bi-linear stress–strain response was noted as FRRP layers increased. Since a ductile post-peak response endeavored, a three-layer hemp FRRP confinement helped achieve this objective. This type of bi-linear behavior has been observed for the case of sufficient CFRP confinement [32]. Confining the cylinders with one and two hemp FRRP layers partially improved the post-peak response, but post-peak strength always reduced as the compressive strain increased. It must be mentioned that a previous study on hemp confinement resulted in a bi-linear response even with single and double hemp FRRP layers [26]. Careful observation of this discrimination would suggest that the type of resin

used must have imparted this difference to the post-peak behavior of one- and two-layer hemp FRRP response. The polyester resin was used in this study as compared to the epoxy resin that was used in earlier work [26].

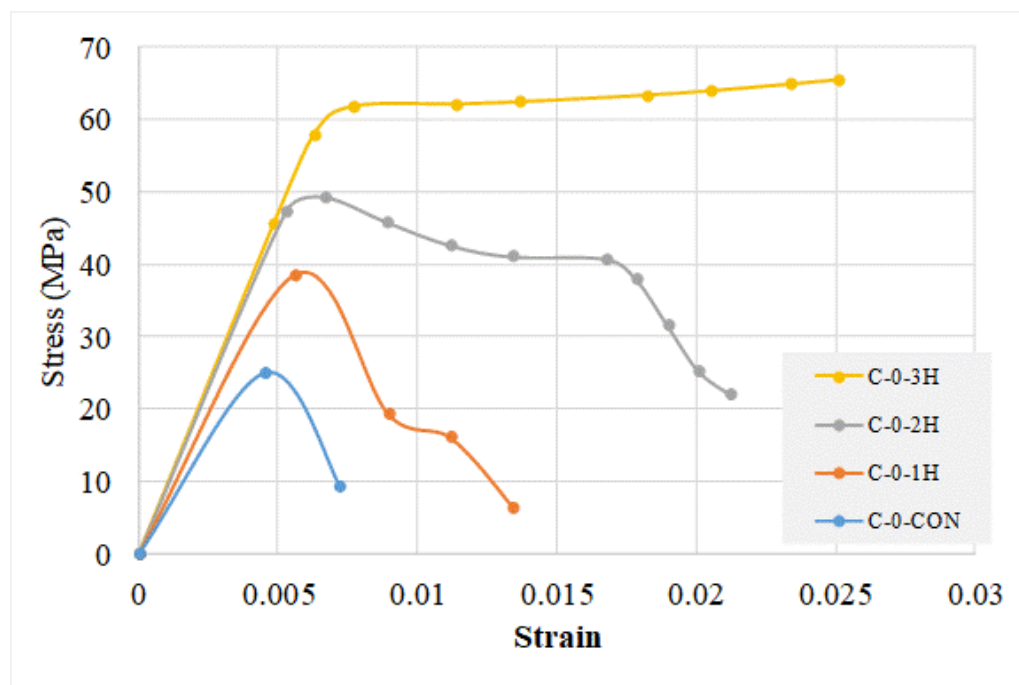


Figure 9. Compressive stress versus strain responses of Group 1 cylinders.

Stress–strain curves for Group 2 cylinders are presented in Figure 10. Analogous to the control cylinder in Group 1 and Group 2 control cylinder also demonstrated a linear increasing branch succeeded by a sudden fall in the axial strength. Group 2 cylinders were constructed by substituting 50% of the natural aggregates with lightweight aggregates. Consequently, their stress–strain behavior exhibited a slightly different response than those of Group 1 cylinders. Though, a similar level of improvement in peak strength and post-peak behavior was demonstrated as the number of hemp FRRP layers increased. A slight drop in the strength was observed next to the peak stress region in the case of two and three FRRP layers. However, cylinders were able to regain their initial peak compressive strength levels. This slight drop in the strength after the peak can be ascribed to the constitutive stress–strain response of polyester resin-coated hemp FRRP that involved a stiff initial branch followed by a slight reduction in stiffness, thus exhibiting a bi-linear response. This transition from the early steep branch to the later softer branch may have resulted in load redistribution, causing a slight drop in peak compressive strength. A previous study [26] on epoxy resin hemp FRRP indicated a linear tensile stress–strain behavior of hemp FRRP. Consequently, such a drop in post-peak compressive strength was not observed.

Finally, the compressive stress–strain response of Group 3 cylinders is presented in Figure 11. To recall, Group 3 cylinders were constructed by substituting 100% of natural aggregates with the lightweight aggregates. The consequence is reflected in their lowest peak strengths among all groups. Furthermore, to compare with Group 2 cylinders, a similar response was observed. An increased number of hemp FRRP layers enhanced the peak strength and improved the post-peak behavior. Analogous to Group 2 cylinders confined with two and three hemp FRRP layers, a slight drop in peak strength was observed, which was quickly regained due to adequate confinement. It can be seen that a single layer of hemp FRRP confinement was insufficient to regain the loss in peak strength.

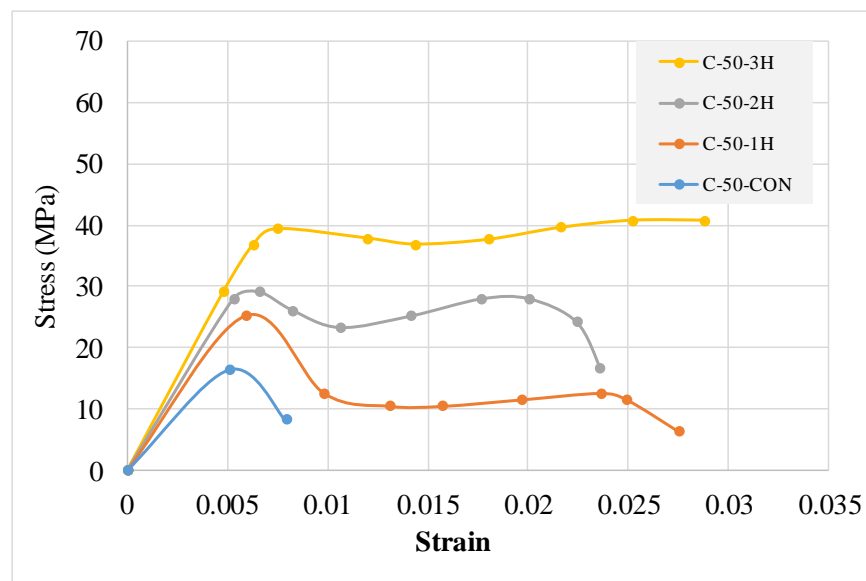


Figure 10. Compressive stress versus strain response of Group 2 cylinders.

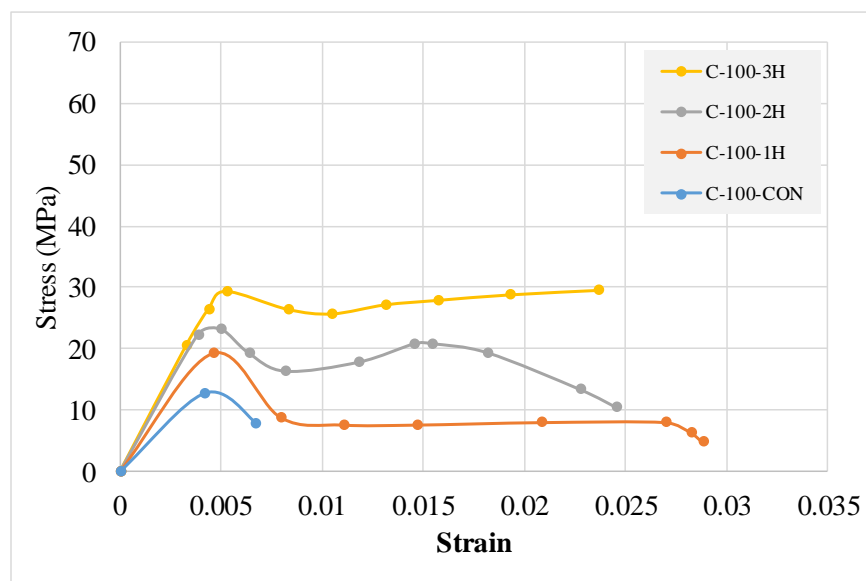
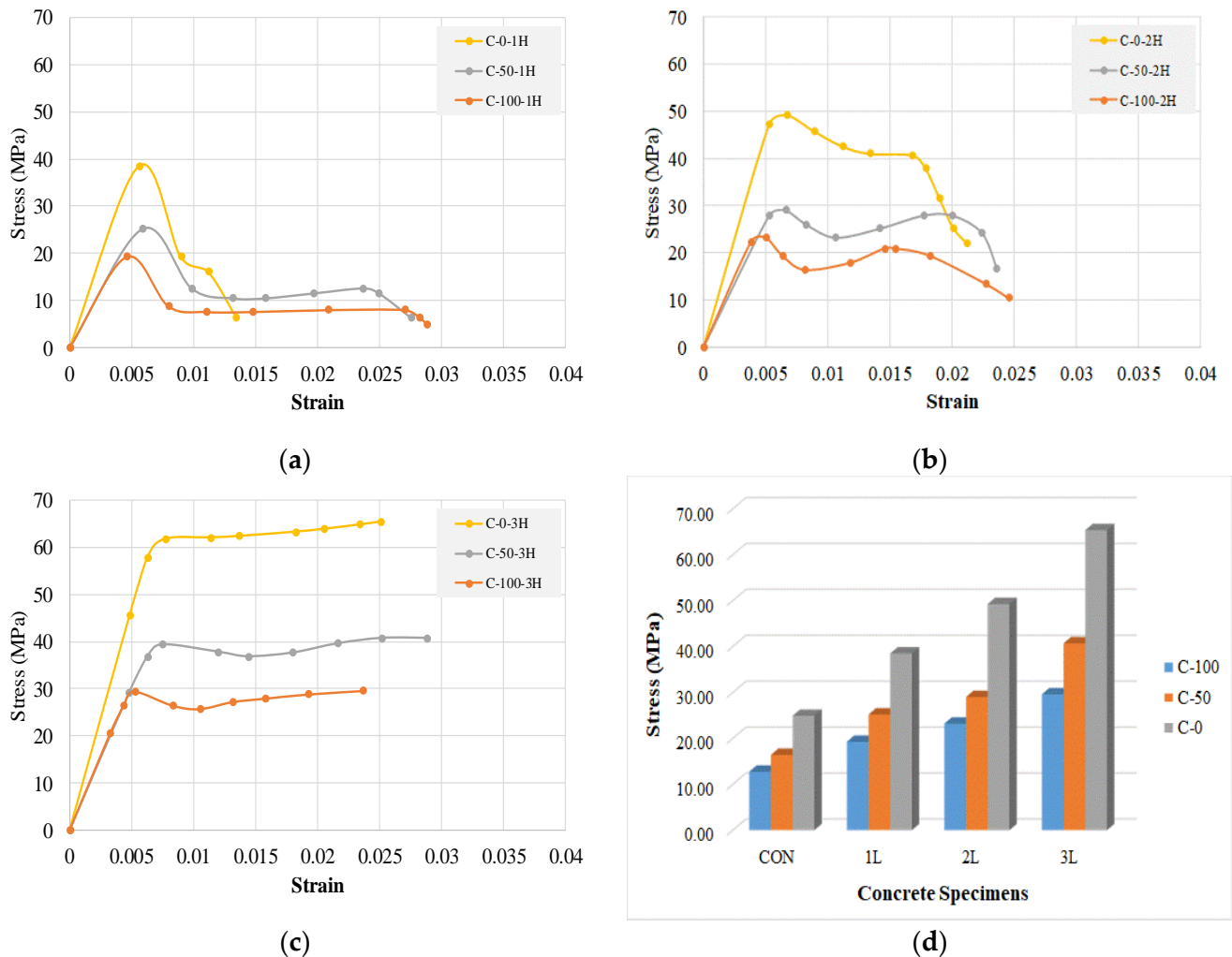


Figure 11. Compressive stress versus strain response of Group 3 cylinders.

### 3.4. Effect of Type of Concrete or Strength of Concrete on Hemp FRP Confinement

Figure 12 presents a comparison between the levels of improvements in peak compressive strengths among cylinders in different groups and confined with the same number of hemp FRP layers. It is evident that a similar level of improvement in the peak stress was noted as FRP layers increased irrespective of the amount of lightweight aggregates. Further to the interest, the shape of the stress—strain response was similar. All cylinders confined with a single FRP layer (see Figure 12a) exhibited a linear ascending branch up until peak strength, followed by a sudden drop in axial capacity. This suggests that a single layer of hemp FRP may be inadequate to impart a ductile post-peak response. For cylinders confined with two layers of hemp FRP and containing lightweight aggregates, a slight drop next to peak compressive strength was observed. However, this drop was closed by the two layers of hemp FRP. This phenomenon was not observed in the case of the cylinder constructed with natural aggregates. A probable reason may suggest that the peak compressive strength of natural aggregate-containing cylinders was highest among all other group cylinders. A two-layer hemp FRP confinement was found to be insufficient

to recover the peak stress after the preliminary post-peak drop. Cylinders confined with three layers of hemp FRRP exhibited a bi-linear stress–strain response (see Figure 12d) irrespective of the presence and amount of lightweight aggregates in the concrete mix. Nonetheless, both the presence and amount of lightweight aggregates reduced the peak strength that could not be recovered irrespective of FRRP layers.



**Figure 12.** Effect of initial concrete strength on the level of improvement, (a) one layer, (b) two layers, (c) three layers and (d) overall comparison.

Figure 13 presents a simplified schematic diagram of the types of stress–strain response obtained for single (SSR-01), double (SSR-02), and three-layer (SSR-03) confined cylinders. SSR-01 response is characterized by a linear step increasing branch succeeded by a sudden drop in the strength. It is noted that points one and three refer to the peak strength and failure strength, respectively. Thus, response types SSR-01 and SSR-03 are characterized by these two points only. For cylinders confined by two hemp FRRP layers, an additional point appears to depict the reduction in the peak stress next to the initial peak, and can be described for the reasons mentioned in earlier sections. It is mentioned that previous studies on hemp FRRP confinement did not result in SSR-02 response, for instance Hussain et al. [30]. In the study by Hussain et al. [30], epoxy resin was utilized to bind hemp ropes to the concrete surface, whereas a polyester resin was used in this study. The stress–strain response in the case of low hemp FRRP confinement also resulted in a bi-linear curve in the study of Hussain et al. [30] that can be attributed to the difference in the mechanical properties of epoxy and polyester resins.

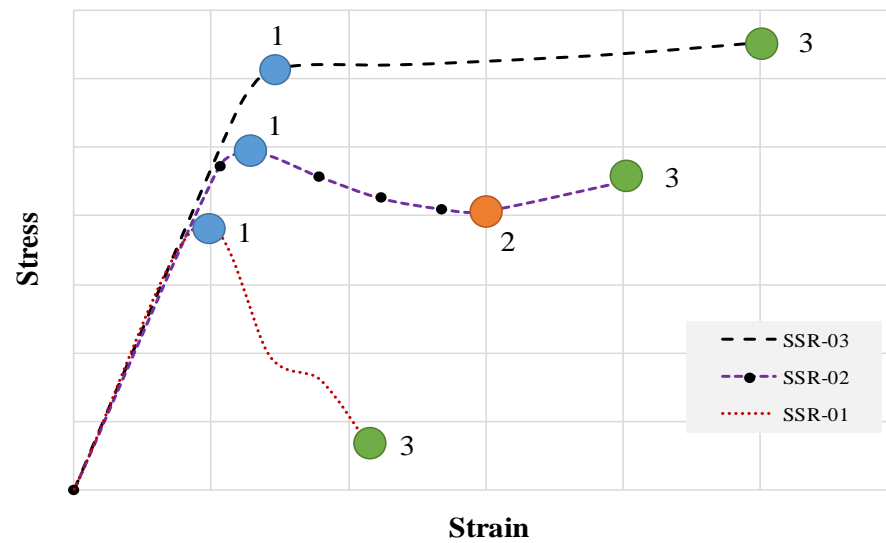


Figure 13. Types of stress–strain response (SSR) observed.

#### 4. Analytical Investigation

The peak stress of the concrete confined with either natural or synthetic FRPs  $f'_{cc}$  is often linked to the compressive strength of unconfined concrete  $f'_{co}$  and external confinement pressure  $f_l$  as:

$$\frac{f'_{cc}}{f'_{co}} = 1 + k_1 \frac{f_l}{f'_{co}} \quad (1)$$

This form of the relation to estimate  $f'_{cc}$  was formulated by Richart et al. [33]. To apply this form of the equation to FRP confinement  $f_l$  is computed from the tensile capacity of FRPs in axial direction and the thickness of FRPs. Thus,  $f_l$  takes the following form.

$$f_l = \frac{2f_{rp}t}{D} \quad (2)$$

where  $f_{rp}$  is the tensile strength and  $t$  is the thickness of FRP wrapped on a cylinder of size  $D$ . To account for multiple FRP layers, Equation (2) is simply multiplied by the number of layers. Some of the peak stress models are listed in Table 4. The application of these models to predict the peak stress of the LWAC strengthened with natural fibers is not yet clear.

Table 4. Existing analytical models.

| Model                     | Expression  | Model                    | Expression   |
|---------------------------|---|--------------------------|--|
| Ghernouti and Rabehi [34] | $\frac{f'_{cc}}{f'_{co}} = 1 + 2.038 \frac{f_l}{f'_{co}}$ | Karbhari and Gao [35]    | $\frac{f'_{cc}}{f'_{co}} = 1 + 2.1 \left( \frac{f_l}{f'_{co}} \right)^{0.87}$  |
| Benzaid et al. [36]       | $\frac{f'_{cc}}{f'_{co}} = 1 + 2.20 \frac{f_l}{f'_{co}}$  | Samaan et al. [37]       | $\frac{f'_{cc}}{f'_{co}} = 1 + 6.0 \frac{f_l^{0.70}}{f'_{co}}$                 |
| Al-Salloum [38]           | $\frac{f'_{cc}}{f'_{co}} = 1 + 2.312 \frac{f_l}{f'_{co}}$ | Miyauchi et al. [39]     | $\frac{f'_{cc}}{f'_{co}} = 1 + 3.50 \frac{f_l}{f'_{co}}$                       |
| Bisby et al. [40]         | $\frac{f'_{cc}}{f'_{co}} = 1 + 2.425 \frac{f_l}{f'_{co}}$ | Saafi et al. [41]        | $\frac{f'_{cc}}{f'_{co}} = 1 + 2.20 \left( \frac{f_l}{f'_{co}} \right)^{0.84}$ |
| Wu et al. [42]            | $\frac{f'_{cc}}{f'_{co}} = 1 + 3.20 \frac{f_l}{f'_{co}}$  | Ilki and Kumbasar [43]   | $\frac{f'_{cc}}{f'_{co}} = 1 + 2.227 \frac{f_l}{f'_{co}}$                      |
| Teng et al. [44]          | $\frac{f'_{cc}}{f'_{co}} = 1 + 3.50 \frac{f_l}{f'_{co}}$  | Spoelstra and Monti [45] | $\frac{f'_{cc}}{f'_{co}} = 0.2 + 3 \left( \frac{f_l}{f'_{co}} \right)^{0.50}$  |
| Richart et al. [33]       | $\frac{f'_{cc}}{f'_{co}} = 1 + 4.10 \frac{f_l}{f'_{co}}$  | Mirmiran [46]            | $\frac{f'_{cc}}{f'_{co}} = 1 + 4.269 \frac{f_l^{0.587}}{f'_{co}}$              |

Table 4. Cont.

| Model               | Expression   | Model                | Expression   |
|---------------------|--|----------------------|--|
| Ahmad and Shah [47] | $\frac{f'_{cc}}{f'_{co}} = 1 + 4.2556 \frac{f_l}{f'_{co}}$ | Pimanmas et al. [48] | $\frac{f'_{cc}}{f'_{co}} = 1 + 3.0 \frac{f_l}{f'_{co}}$  |
| Hussain et al. [49] | $\frac{f'_{cc}}{f'_{co}} = 1 + 6.40 \frac{f_l}{f'_{co}}$   | Yan [50]             | $\frac{f'_{cc}}{f'_{co}} = 1 + 1.86 \frac{f_l}{f'_{co}}$ |

Figure 14a presents a comparison among the analytical and experimental peak stresses of Group 1 cylinders confined with hemp FRRP. All models underestimated the peak stresses except the model of Hussain et al. [49]. The scatter of the analytical predictions intensified as the FRRP confinement improved. For cylinders fabricated with 50% lightweight aggregates, their analytical predictions are shown in Figure 14b. The mean of the predictions of analytical models was close to the experimental values. Finally, most of the models overestimated the experimental strengths when the lightweight aggregate amount was increased to 100% (see Figure 14c).

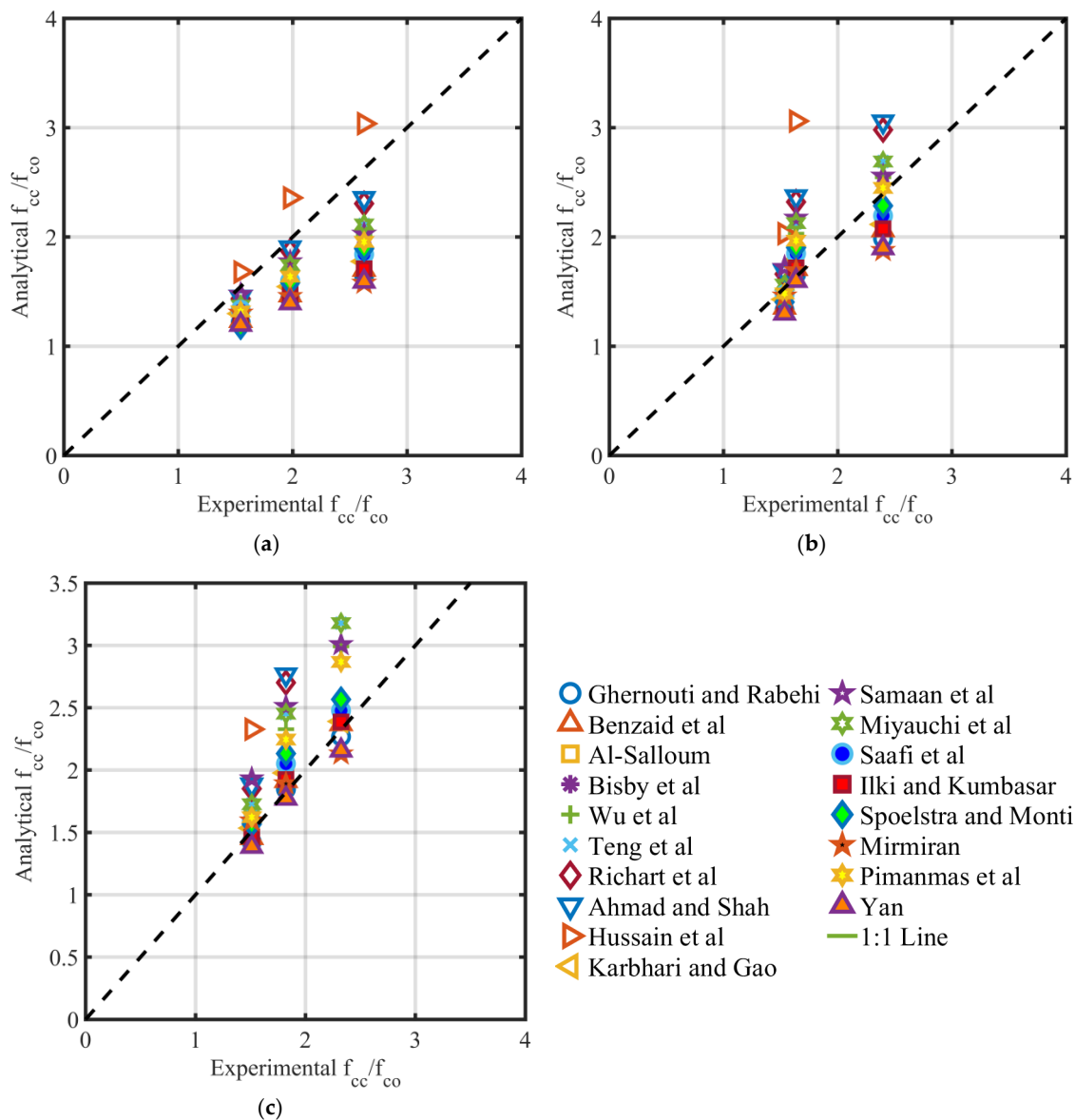


Figure 14. Comparison of analytical vs. experimental compressive strength of hemp FRRP confined cylinders (a) Group 1 (b) Group 2, and (c) Group 3.

The performance of the considered models against the test database of this study is assessed using the average absolute error (AAR%) and average ratio (AR). The AAR gives an estimation of the mean of the absolute estimate of the difference between the predicted and experimentally observed value, whereas AR gives an average value describing the degree of overestimation or underestimation corresponding to the model's prediction. AAR and AR are determined from Equations (3) and (4), respectively [51].

$$AAR = \frac{\sum_{i=1}^N \left| \frac{\text{Theoretical} - \text{Experimental}}{\text{Theoretical}} \right|}{N} \quad (3)$$

$$AR = \frac{\sum_{i=1}^N \frac{\text{Theoretical}}{\text{Experimental}}}{N} \quad (4)$$

where  $N$  stands for the number of total data points. Table 5 presents the summary of AAR and AR values calculated against each considered analytical model. AR values for models are plotted in Figure 15. Figure 15 provides the upper and lower thresholds corresponding to a 5% variation from the experimental results. To clarify, areas above and below those thresholds are filled with different colors. As seen in Figure 15a, no model was able to predict reasonable estimates of experimental results corresponding to Group 1 cylinders. Figure 15b provides AR values corresponding to the experimental results of Group 2 cylinders. In this category, the models of Bisby et al. [40], Karbhari and Gao [35], Saafi et al. [41], Ilki and Kumbasar [43], and Spoelstra and Monti [45] were able to provide estimates within the adopted thresholds. Finally, reasonable AR estimates for Group 3 cylinders included the models of Ghernouti and Rabehi [34], Benzaid et al. [36], Al-Salloum [38], Ilki and Kumbasar [43], and Mirmiran et al. [46]. It can be noted that none of the peak stress models demonstrated consistency in predicting accurate compressive strengths of the cylinders in all three groups. Therefore, a further need to enhance the experimental record of hemp FRRP confined lightweight aggregate concrete is first identified. With such an adequate database, the availability of a reasonable analytical model can be ensured.

**Table 5.** Assessment of existing ultimate strain models.

| Model                     | 0% Light-Weight Aggregates |      | 50% Light-Weight Aggregates |      | 100% Light-Weight Aggregates |      |
|---------------------------|----------------------------|------|-----------------------------|------|------------------------------|------|
|                           | AAE (%)                    | AR   | AAE (%)                     | AR   | AAE (%)                      | AR   |
| Ghernouti and Rabehi [34] | 29                         | 0.71 | 11                          | 0.90 | 4                            | 0.97 |
| Benzaid et al. [36]       | 27                         | 0.72 | 10                          | 0.93 | 4                            | 1.01 |
| Al-Salloum [38]           | 26                         | 0.74 | 10                          | 0.95 | 5                            | 1.03 |
| Bisby et al. [40]         | 25                         | 0.75 | 9                           | 0.97 | 6                            | 1.05 |
| Wu et al. [42]            | 30                         | 0.83 | 11                          | 1.10 | 22                           | 1.22 |
| Teng et al. [44]          | 14                         | 0.86 | 15                          | 1.15 | 29                           | 1.28 |
| Richart et al. [33]       | 8                          | 0.92 | 25                          | 1.25 | 41                           | 1.41 |
| Ahmad and Shah [47]       | 7                          | 0.93 | 27                          | 1.27 | 45                           | 1.44 |
| Hussain et al. [49]       | 15                         | 1.14 | 64                          | 1.64 | 90                           | 1.90 |
| Karbhari and Gao [35]     | 23                         | 0.77 | 9                           | 0.97 | 4                            | 1.04 |
| Samaan et al. [37]        | 13                         | 0.87 | 17                          | 1.17 | 31                           | 1.31 |
| Miyauchi et al. [39]      | 14                         | 0.86 | 15                          | 1.15 | 29                           | 1.29 |
| Saafi et al. [41]         | 21                         | 0.79 | 9                           | 1.00 | 8                            | 1.08 |
| Ilki and Kumbasar [43]    | 27                         | 0.73 | 10                          | 0.93 | 4                            | 1.02 |
| Spoelstra and Monti [45]  | 24                         | 0.76 | 10                          | 1.01 | 10                           | 1.10 |

Table 5. Cont.

| Model                | 0% Light-Weight Aggregates |      | 50% Light-Weight Aggregates |      | 100% Light-Weight Aggregates |      |
|----------------------|----------------------------|------|-----------------------------|------|------------------------------|------|
|                      | AAE (%)                    | AR   | AAE (%)                     | AR   | AAE (%)                      | AR   |
| Mirmiran [46]        | 27                         | 0.72 | 10                          | 0.92 | 6                            | 1.00 |
| Pimanmas et al. [48] | 19                         | 0.81 | 9                           | 1.06 | 18                           | 1.18 |
| Yan [50]             | 31                         | 0.69 | 13                          | 0.87 | 6                            | 0.93 |

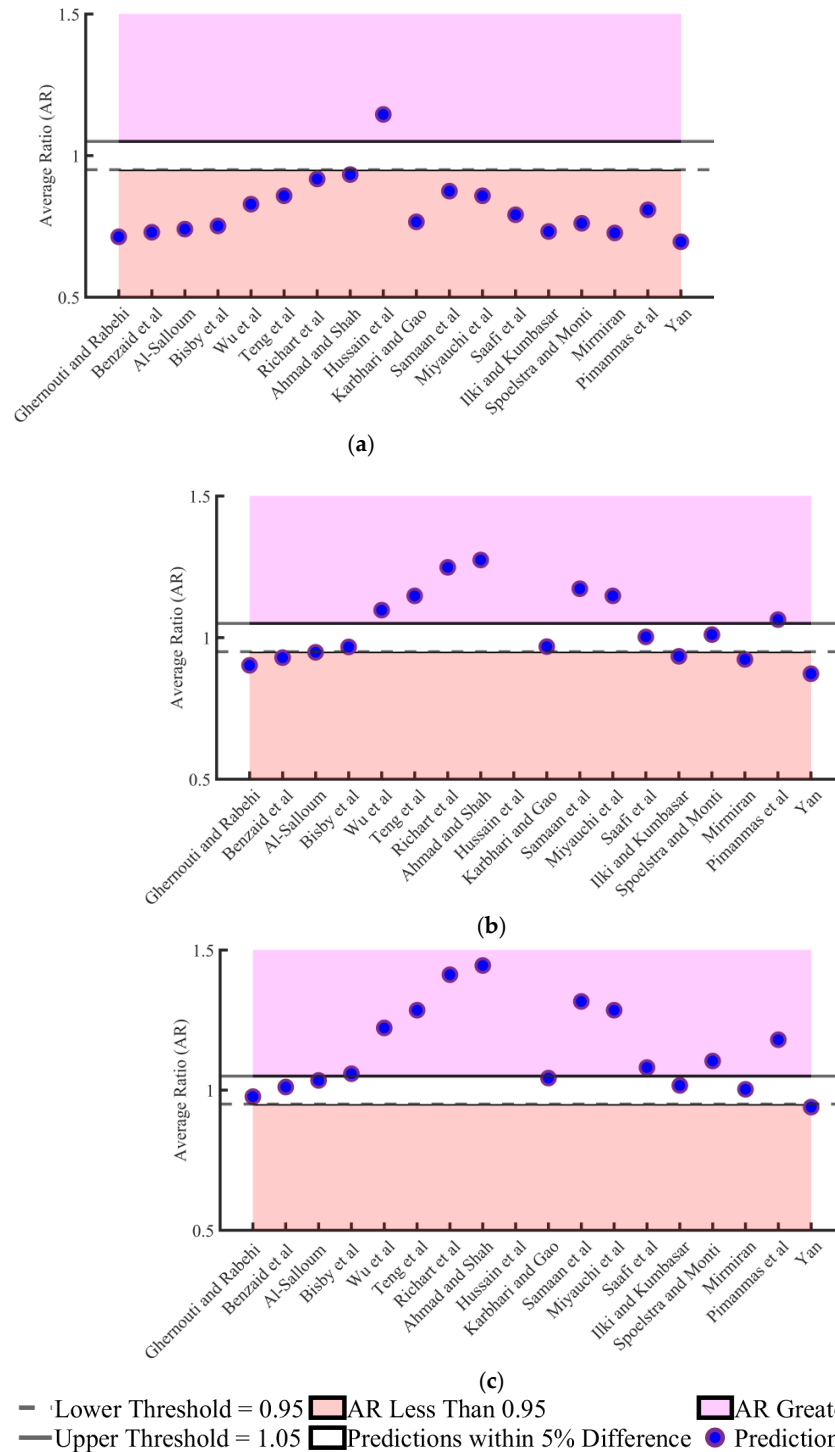


Figure 15. Average ratios of analytical models for (a) Group 1 (b) Group 2, and (c) Group 3 [33–50].

## 5. Discussion

Strengthening of lightweight aggregate concrete (LWAC) is usually accomplished by wrapping the synthetic FRP jackets around LWAC. The cost of synthetic FRPs is about 180 USD/m<sup>2</sup> [52]. On the contrary, the price of hemp FRRP is about 7 USD/kg, whereas approximately 67 m of hemp rope is available per kilogram. A substantial reduction in the price of hemp FRRP as compared to the synthetic FRP is evident. Dabbagh et al. [2] strengthened cylinders of size 150 mm × 300 mm using one, two, three, and four layers of the CFRP jackets. A single CFRP layer increased the peak strength of LWAC by 42.1%. The surface area of the cylinders was same as those tested in the present study and estimated at 141,300 mm<sup>2</sup>. This required CFRP of about 0.14 m<sup>2</sup> or an equivalent cost of about 25 USD. A single layer of hemp FRRP increased the peak strength by 55% in this study. The nominal diameter of hemp FRRP was 2.2 mm. To cover the height of 300 mm, roughly 64 m of hemp FRRP was required corresponding to a cost of about 7 USD, which is 257% lower than the cost of the CFRP jacket. It is pertinent to mention that the application of hemp FRRP to the full-scale members can be performed using rope wrapping machines to speed up the process.

As discussed in the Section 1, no experimental work is yet conducted to assess the effectiveness of hemp fiber ropes in the strengthening of LWAC. Further to Section 3.4, the compressive strength of the control specimens degraded as the replacement ratio of the natural aggregates is increased. The compressive strength of Specimen C-0-CON was 24.90 MPa. When the replacement ratio was 50%, two layers of hemp fiber ropes increased the compressive strength to 26.83 MPa. This suggests that the substandard compressive strength of LWAC was enhanced up to the level of the natural aggregate concrete by two hemp rope layers when the replacement ratio was 50%. Whereas, it took three hemp rope layers to enhance the compressive strength of LWAC beyond the level of the natural aggregate concrete when the replacement ratio was 100%. In view of this, it is suggested to use at least three layers of hemp ropes to match the compressive strength of natural aggregate concrete with similar concrete mix proportions. For the ultimate strain, a single layer of hemp rope was enough to increase the ultimate strain beyond 0.0045 that was the threshold set by Specimen C-0-CON, i.e., control specimen of the natural aggregate concrete. The ultimate strain of three-layer confinement in three groups was similar. However, the experimental results suggest that a higher hemp rope confinement than a three-layer would be required to increase the compressive strength to the level the natural aggregate concrete. This is evident from Table 3 as Specimen C-0-3H sustained a compressive strength of 65.34 MPa, whereas the compressive strengths of Specimens C-50-3H and C-100-3H were 39.33 MPa and 29.58 MPa, respectively.

## 6. Conclusions

This study recognizes the deficient intrinsic properties of lightweight aggregate concrete (LWAC) and proposes a sustainable solution using natural hemp fiber-reinforced rope polymers (FRRPs). Compressive stress–strain response of 24-cylinder specimens is presented. To characterize the presence of lightweight aggregates quantitatively, cylinders were tested in three different groups. Cylinders in Groups 1, 2, and 3 cylinders were fabricated by replacing 0%, 50%, and 100% of the natural aggregates with the lightweight aggregates, respectively. The following important results can be deduced:

1. The ultimate failure mode of control cylinders (i.e., without hemp FRRP confinement) was typical, comprising crushing and splitting. However, the failure cone of the control cylinder in Group 2 was found to have its apex shifted towards the top. It was recognized that partial replacement of natural aggregates might have created aggregate density segregation during compaction. The issue of segregation must be accounted for and good care must be taken during the mixing and pouring of the concrete with partial replacement of natural aggregates as it may further deteriorate the mechanical properties of LWAC and undermine the efficacy of hemp FRRP wraps.

2. The peak stress was reduced by 34% and 49% in the presence of 50% and 100% of lightweight aggregates, respectively. The peak stress of cylinders in all three groups was found to have a positive trend with FRRP layers. The peak stress of lightweight aggregate concrete could not achieve the same strength as those of Group 1 cylinders in the presence of hemp FRRP confinement.
3. It was found that cylinders in Groups 2 and 3 demonstrated peak stresses of 25.18 and 23.20 MPa for one and two layers of hemp FRRP confinement. The peak stress of the Group 1 control cylinder was 24.90 MPa. It is interesting to observe that one layer of hemp FRRP on Group 2 cylinders (i.e., 50% aggregate replacement) was sufficient to enhance the peak stress to the same level as that of the control cylinder in Group 1 (i.e., fabricated using natural aggregates only). In contrast, it took two layers of the external FRRP on Group 3 cylinders to achieve the same strength. Therefore, it is recommended to use at least three hemp FRRP layers to obtain the optimal results irrespective of the quantity of lightweight aggregates until further data become available. Further, a three-layer confinement resulted in a bi-linear stress–strain response irrespective of the number of hemp FRRP wraps. Based on the previous studies [32,53], a bi-linear response can be associated with sufficient confinement.
4. Several existing models were evaluated to calculate the peak stress of hemp FRRP confined LWAC concrete. Few of those models were able to predict satisfactory estimates of the experimental results. However, their consistency in predicting the peak stress of all three groups was highly questionable. Therefore, further studies are required to increase the database of natural FRRP confined LWAC. With a reasonable sample size, an adequate analytical model can then be proposed in the future research.
5. For a similar increase in the peak compressive stress, the cost of hemp FRRP was about 257% lower than the cost of the CFRP sheet. The conclusion was drawn by comparing an existing study on the strengthening of LWAC with similar cylinder dimensions using CFRP sheets.

**Author Contributions:** Conceptualization, S.S. and P.J.; Data curation, N.A. and C.K.G.; Formal analysis, K.C. and M.A.J.; Investigation, N.A.; Methodology, E.Y. and Q.H.; Resources, A.W.A.Z.; Visualization, K.C., A.W.A.Z., E.Y. and M.A.J.; Writing—original draft, S.S. and P.J.; Writing—review & editing, S.S., C.K.G., Q.H., P.J. and M.A.J. All authors have read and agreed to the published version of the manuscript.

**Funding:** This research was funded by the Faculty of Engineering, Srinakharinwirot University, Thailand (Research Grant ID 192/2564).

**Institutional Review Board Statement:** Not applicable.

**Acknowledgments:** The authors of this research work are very grateful to the Faculty of Engineering, Srinakharinwirot University, Thailand, for providing research grant (Research Grant ID 192/2564) to carry out the research work. Thanks are also extended to the Siam City Cement Public Company Limited, Thailand for providing materials for this research. Thanks are also extended to the Research and Innovation Development Unit for Infrastructure and Rail Transportation Structural System (RIDIR), Srinakharinwirot University, Nakhonnayok, Thailand for supporting this research. The authors also like to extend their gratitude to the Asian Institute of Technology (AIT) for supporting test facilities.

**Conflicts of Interest:** The authors declare no conflict of interest.

## Abbreviations

|      |   |
|------|---|
| AAR  | Average absolute error                  |
| AR   | Average ratio                           |
| FRP  | Fiber-reinforced polymer                |
| FRRP | Fiber reinforced rope polymer           |
| LVDT | Linear variable differential transducer |
| LWAC | Lightweight aggregate concrete          |

|           |  |
|-----------|--|
| NAC       | Natural aggregate concrete                         |
| RAC       | Recycled aggregate concrete                        |
| UTM       | Universal testing machine                          |
| $D$       | Diameter of cylinder                               |
| $f'_{cc}$ | Peak compressive stress of confined concrete       |
| $f_{co}$  | Unconfined concrete compressive strength           |
| $f_l$     | Lateral confinement pressure                       |
| $f_{frp}$ | Tensile strength of hemp FRRP sheet                |
| $k_1$     | Constant of regression for peak compressive stress |
| $n_f$     | Number of FRRP sheets                              |
| $t$       | Thickness of FRRP sheet                            |

## References

1. Kucharczyková, B.; Keršner, Z.; Pospíchal, O.; Misák, P.; Vymazal, T. Influence of freeze—Thaw cycles on fracture parameters values of lightweight concrete. *Procedia Eng.* **2010**, *2*, 959–966. [[CrossRef](#)]
2. Dabbagh, H.; Delshad, M.; Amoozazei, K. Design-Oriented Stress-Strain Model for FRP-Confined Lightweight Aggregate Concrete. *KSCE J. Civ. Eng.* **2021**, *25*, 219–234. [[CrossRef](#)]
3. Lim, J.C.; Ozbakkaloglu, T. Stress–strain model for normal-and light-weight concretes under uniaxial and triaxial compression. *Constr. Build. Mater.* **2014**, *71*, 492–509. [[CrossRef](#)]
4. Melby, K.; Jordet, E.A.; Hansvold, C. Long-span bridges in Norway constructed in high-strength LWA concrete. *Eng. Struct.* **1996**, *18*, 845–849. [[CrossRef](#)]
5. Haug, A.K.; Fjeld, S. A floating concrete platform hull made of lightweight aggregate concrete. *Eng. Struct.* **1996**, *18*, 831–836. [[CrossRef](#)]
6. Rossignolo, J.A.; Agnesini, M.V.C.; Morais, J.A. Properties of high-performance LWAC for precast structures with Brazilian lightweight aggregates. *Cem. Concr. Compos.* **2003**, *25*, 77–82. [[CrossRef](#)]
7. Yasar, E.; Atis, C.D.; Kilic, A.; Gulsen, H. Strength properties of lightweight concrete made with basaltic pumice and fly ash. *Mater. Lett.* **2003**, *57*, 2267–2270. [[CrossRef](#)]
8. Zhou, Y.; Liu, X.; Xing, F.; Cui, H.; Sui, L. Axial compressive behavior of FRP-confined lightweight aggregate concrete: An experimental study and stress-strain relation model. *Constr. Build. Mater.* **2016**, *119*, 1–15. [[CrossRef](#)]
9. Wang, H.T.; Wang, L.C. Experimental study on static and dynamic mechanical properties of steel fiber reinforced lightweight aggregate concrete. *Constr. Build. Mater.* **2013**, *38*, 1146–1151. [[CrossRef](#)]
10. Holm, T.A.; Bremner, T.W. Durability of Structural Lightweight Concrete. *Spec. Publ.* **1991**, *126*, 1119–1134. [[CrossRef](#)]
11. Wei, H.; Wu, T.; Liu, X.; Zhang, R. Investigation of stress-strain relationship for confined lightweight aggregate concrete. *Constr. Build. Mater.* **2020**, *256*, 119432. [[CrossRef](#)]
12. Khaloo, A.R.; El-Dash, K.M.; Ahmad, S.H. Model for Lightweight Concrete Columns Confined by Either Single Hoops or Interlocking Double Spirals. *Struct. J.* **1999**, *96*, 883–890. [[CrossRef](#)]
13. Jiang, J.; Zhang, Z.; Fu, J.; Ramakrishnan, K.R.; Wang, C.; Wang, H. Impact damage behavior of lightweight CFRP protection suspender on railway vehicles. *Mater. Des.* **2022**, *213*, 110332. [[CrossRef](#)]
14. Dai, J.-G.; Bai, Y.-L.; Teng, J.G. Behavior and Modeling of Concrete Confined with FRP Composites of Large Deformability. *J. Compos. Constr.* **2011**, *15*, 963–973. [[CrossRef](#)]
15. Wenchen, M. Simulate Initiation and Formation of Cracks and Potholes. Master's Thesis, Northeastern University, Boston, MA, USA, 2016.
16. Wenchen, M. Behavior of Aged Reinforced Concrete Columns Under High Sustained Concentric and Eccentric Loads. Ph.D. Thesis, University of Nevada, Reno, NV, USA, 2021.
17. Li, P.; Wu, Y.F.; Gravina, R. Cyclic response of FRP-confined concrete with post-peak strain softening behavior. *Constr. Build. Mater.* **2016**, *123*, 814–828. [[CrossRef](#)]
18. Li, P.; Wu, Y.F. Stress–strain behavior of actively and passively confined concrete under cyclic axial load. *Compos. Struct.* **2016**, *149*, 369–384. [[CrossRef](#)]
19. Li, P.; Wu, Y.F. Stress–strain model of FRP confined concrete under cyclic loading. *Compos. Struct.* **2015**, *134*, 60–71. [[CrossRef](#)]
20. Triantafillou, T.C.; Papanicolaou, C.G.; Zissimopoulos, P.; Laourdekis, T. Concrete Confinement with Textile-Reinforced Mortar Jackets. *Struct. J.* **2006**, *103*, 28–37. [[CrossRef](#)]
21. Minamoto, K.; Nagano, M.; Inaoka, T.; Kitano, T.; Ushijima, K.; Fukuda, Y.; Futatsuka, M. Skin problems among fiber-glass reinforced plastics factory workers in Japan. *Ind. Health* **2002**, *40*, 42–50. [[CrossRef](#)]
22. Tarvainen, K.; Jolanki, R.; Forsman-Grönholm, L.; Estlander, T.; Pfäffli, P.; Juntunen, J.; Kanerva, L. Exposure, skin protection and occupational skin diseases in the glass-fibre-reinforced plastics industry. *Contact Dermat.* **1993**, *29*, 119–127. [[CrossRef](#)]
23. Tarvainen, K.; Jolanki, R.; Estlander, T. Occupational contact allergy to unsaturated polyester resin cements. *Contact Dermat.* **1993**, *28*, 220–224. [[CrossRef](#)] [[PubMed](#)]
24. Wahlberg, J.E.; Wrangsjö, K. Is cobalt naphthenate an allergen? *Contact Dermat.* **1985**, *12*, 225. [[CrossRef](#)] [[PubMed](#)]

25. Shalabi, F.I.; Mazher, J.; Khan, K.; Alsuliman, M.; Alm Mustafa, I.; Mahmoud, W.; Alomran, N. Cement-stabilized waste sand as sustainable construction materials for foundations and highway roads. *Materials* **2019**, *12*, 600. [[CrossRef](#)] [[PubMed](#)]
26. Hussain, Q.; Ruangrassamee, A.; Tangtermsirikul, S.; Joyklad, P. Behavior of concrete confined with epoxy bonded fiber ropes under axial load. *Constr. Build. Mater.* **2020**, *263*, 120093. [[CrossRef](#)]
27. Suparp, S.; Ali, N.; al Zand, A.W.; Chaiyasarn, K.; Rashid, M.U.; Yooprasertchai, E.; Hussain, Q.; Joyklad, P. Axial Load Enhancement of Lightweight Aggregate Concrete (LAC) Using Environmentally Sustainable Composites. *Buildings* **2022**, *12*, 851. [[CrossRef](#)]
28. Hussain, Q.; Ruangrassamee, A.; Joyklad, P.; Wijeyewickrema, A.C. Shear Enhancement of RC Beams Using Low-Cost Natural Fiber Rope Reinforced Polymer Composites. *Buildings* **2022**, *12*, 602. [[CrossRef](#)]
29. Joyklad, P.; Yooprasertchai, E.; Rahim, A.; Ali, N.; Chaiyasarn, K.; Hussain, Q. Sustainable and Low-Cost Hemp FRP Composite Confinement of B-Waste Concrete. *Sustainability* **2022**, *14*, 7673. [[CrossRef](#)]
30. Hussain, Q.; Ruangrassamee, A.; Tangtermsirikul, S.; Joyklad, P.; Wijeyewickrema, A.C. Low-Cost Fiber Rope Reinforced Polymer (FRRP) Confinement of Square Columns with Different Corner Radii. *Buildings* **2021**, *11*, 355. [[CrossRef](#)]
31. EIHA. The European Hemp Industry Association. In Proceedings of the 17th Hemp Conference, Duesseldorf, Germany, 16–17 June 2021.
32. Sadeghian, P.; Rahai, A.R.; Ehsani, M.R. Numerical Modeling of Concrete Cylinders Confined with CFRP Composites. *J. Reinf. Plast. Compos.* **2008**, *27*, 1309–1321. [[CrossRef](#)]
33. Richart, F.E.; Brandtzaeg, A.; Brown, R.L. *A Study of the Failure of Concrete under Combined Compressive Stresses*; Bulletins—Engineering Experiment Station: Bryan, TX, USA, 1928. Available online: <http://hdl.handle.net/2142/4277> (accessed on 6 March 2022).
34. Ghernouti, Y.; Rabehi, B. FRP-confined short concrete columns under compressive loading: Experimental and modeling investigation. *J. Reinf. Plast. Compos.* **2010**, *30*, 241–255. [[CrossRef](#)]
35. Karbhari, V.M.; Gao, Y. Composite Jacketed Concrete under Uniaxial Compression—Verification of Simple Design Equations. *J. Mater. Civ. Eng.* **1997**, *9*, 185–193. [[CrossRef](#)]
36. Benzaid, R.; Mesbah, H. Nasr Eddine Chikh, FRP-confined Concrete Cylinders: Axial Compression Experiments and Strength Model. *J. Reinf. Plast. Compos.* **2010**, *29*, 2469–2488. [[CrossRef](#)]
37. Samaan, M.; Mirmiran, A.; Shahawy, M. Model of Concrete Confined by Fiber Composites. *J. Struct. Eng.* **1998**, *124*, 1025–1031. [[CrossRef](#)]
38. Al-Salloum, Y.A. Compressive strength models of FRP-confined concrete. In Proceedings of the 1st Asia-Pacific Conference on FRP in Structures: APFIS 2007, Hong Kong, China, 12–14 December 2007; ePublications@SCU: Lismore, Australia, 2007; Volume 1, pp. 175–180.
39. Miyauchi, K. Estimation of Strengthening Effects with Carbon Fiber Sheet for Concrete Column. In Proceedings of the 3rd International Symposium on Non-Metallic (FRP) Reinforcement for Concrete Structures, Sapporo, Japan, 14–16 October 1997; Japan Concrete Institute: Tokyo, Japan; pp. 217–224. Available online: <https://ci.nii.ac.jp/naid/80009963999/> (accessed on 6 March 2022).
40. Bisby, L.A.; Dent, A.J.S.; Green, M.F. Comparison of confinement models for fiber-reinforced polymer-wrapped concrete. *ACI Struct. J.* **2005**, *102*, 62–72. [[CrossRef](#)]
41. Saafi, M.; Toutanji, H.A.; Li, Z. Behavior of concrete columns confined with fiber reinforced polymer tubes. *ACI Mater. J.* **1999**, *96*, 500–509. [[CrossRef](#)]
42. Wu, H.-L.; Wang, Y.-F.; Yu, L.; Li, X.-R. Experimental and Computational Studies on High-Strength Concrete Circular Columns Confined by Aramid Fiber-Reinforced Polymer Sheets. *J. Compos. Constr.* **2009**, *13*, 125–134. [[CrossRef](#)]
43. Ilki, A.; Kumbasar, N. Behavior of damaged and un-damaged concrete strengthened by carbon fiber composite sheets. *Int. J. Struct. Eng. Mech* **2002**, *13*, 75–90. [[CrossRef](#)]
44. Teng, J.G.; Huang, Y.L.; Lam, L.; Ye, L.P. Theoretical Model for Fiber-Reinforced Polymer-Confined Concrete. *J. Compos. Constr.* **2007**, *11*, 201–210. [[CrossRef](#)]
45. Spoelstra, M.R.; Monti, G. FRP-Confined Concrete Model. *J. Compos. Constr.* **1999**, *3*, 143–150. [[CrossRef](#)]
46. Mirmiran, A.; Shahawy, M. Behavior of Concrete Columns Confined by Fiber Composites. *J. Struct. Eng.* **1997**, *123*, 583–590. [[CrossRef](#)]
47. Ahmad, S.H.; Shah, S.P. Complete Triaxial Stress-Strain Curves for Concrete. *J. Struct. Div.* **1982**, *108*, 728–742. [[CrossRef](#)]
48. Pimanmas, A.; Hussain, Q.; Panyasirikhunawut, A.; Rattanapitikon, W. Axial strength and deformability of concrete confined with natural fibre-reinforced polymers. *Mag. Concr. Res.* **2018**, *71*, 55–70. [[CrossRef](#)]
49. Hussain, Q.; Rattanapitikon, W.; Pimanmas, A. Axial load behavior of circular and square concrete columns confined with sprayed fiber-reinforced polymer composites. *Polym. Compos.* **2016**, *37*, 2557–2567. [[CrossRef](#)]
50. Yan, L. Plain concrete cylinders and beams externally strengthened with natural flax fabric reinforced epoxy composites. *Mater. Struct. /Mater. Et Constr.* **2016**, *49*, 2083–2095. [[CrossRef](#)]
51. Pimanmas, A.; Saleem, S. Evaluation of Existing Stress–Strain Models and Modeling of PET FRP-Confined Concrete. *J. Mater. Civ. Eng.* **2019**, *31*, 04019303. [[CrossRef](#)]

- 
52. Mumtaz, Y.; Nasiri, A.; Tetsuhiro, S. A comparative study on retrofitting concrete column by FRP-Wrapping and RC-Jacketing methods: A feasibility study for Afghanistan. *Indian J. Sci. Technol.* **2021**, *14*, 652–664. [[CrossRef](#)]
  53. Harajli, M.H. Axial stress–strain relationship for FRP confined circular and rectangular concrete columns. *Cem. Concr. Compos.* **2006**, *28*, 938–948. [[CrossRef](#)]